Mon. Not. R. Astron. Soc. **000**, 1–12 (2004) Printed 5 February 2008 (MN LaTeX style file v2.2)

Elemental abundances in the Blanco 1 open cluster

A. Ford[1], R.D. Jeffries[2] and B. Smalley[2]
[1] *CSPA/SPME, Building 28M, Monash University, VIC 3800, Australia*
[2] *Astrophysics Group, School of Chemistry and Physics, Keele University, Keele, Staffordshire ST5 5BG, United Kingdom*

Submitted August 2005

ABSTRACT
High resolution spectroscopy is used to determine the detailed chemical abundances of a group of eight F- and G-type stars in the young open cluster Blanco 1. An average [Fe/H] of +0.04 ±0.02 (internal error) ±0.04 (external error) is found, considerably lower than a previous spectroscopic estimate for this cluster. The difference is due mainly to our adoption of significantly cooler temperatures which are consistent with both photometric and spectroscopic constraints. Blanco 1 exhibits sub-solar [Ni/Fe] (−0.18 ±0.01 ±0.01), [Si/Fe] (−0.09 ±0.02 ±0.03), [Mg/Fe] (−0.14 ±0.02 ±0.03) and [Ca/Fe] (−0.09 ±0.03 ±0.03); ratios which are not observed among nearby field stars. The material from which Blanco 1 formed may not have been well mixed with interstellar matter in the galactic disc, which tallies with its current location about 240 pc below the galactic plane. A simultaneous deficit of Ni and alpha elements with respect to Fe is hard to reconcile with most published models of yields from supernovae of types Ia and II. The revised abundances for Blanco 1 indicate that overall radiative opacities in its stars, and hence convective zone properties at a given mass, are similar to those in the Pleiades at approximately the same age. This can explain a previous observation that the Li depletion patterns of G- and K-type stars in the two clusters are indistinguishable. The lower overall metallicity of Blanco 1 now make it less attractive as a target for discovering transiting, short period exoplanets.

Key words: stars: abundances – stars: late-type – open clusters and associations: individual: Blanco 1

1 INTRODUCTION

Open clusters are excellent laboratories for testing our understanding of stellar structure. Their numerous stars share common ages and distances, reducing many uncertainties associated with field-star studies. Abundances for elements other than Fe and Li are rarely available in open clusters, yet these have a profound bearing on stellar structure calculations.

A case in point is the Blanco 1 cluster which has an age similar to, or a little younger than, the Pleiades (50-100 Myr – Perry, Walter & Crawford; Panagi et al. 1994). Edvardsson et al. (1995, hereafter E95) claimed [Fe/H] =+0.23 for the cluster on the basis of spectroscopy of several F stars. E95 discussed this high metallicity in terms of the unusual location of Blanco 1. The cluster is 240 pc below the galactic plane and may have crossed the plane on one or more occasions. The apparent metal-rich status of the cluster has lead to a number of investigations that have sought to isolate the composition dependence of various physical phenomena. Pillitteri et al. (2003, 2004) have used Blanco 1 to determine whether metallicity influences the coronal X-ray losses from low-mass stars with convective envelopes. Blanco 1 may well be a fruitful location to search for transiting exoplanets, given the established relationship between stellar metallicity and the frequency of short-period exoplanets around field stars (e.g. Santos, Israelian & Mayor 2004 and references therein).

Jeffries & James (1999, hereafter JJ99) found that the Li depletion pattern with $T_{\rm eff}$ among the G/K stars of Blanco 1 could not be distinguished from the similarly aged Pleiades, which has [Fe/H]= −0.03 (Boesgaard & Friel 1990). This result contradicts the strong metallicity dependence predicted by models of pre-main-sequence (PMS) Li depletion, implying that some unknown mechanism inhibits PMS Li depletion in the Blanco 1 stars and that some non-convective mixing process operates in main sequence stars to ensure that Li-depletion in a metal-rich ZAMS cluster like Blanco 1 could approach that seen in the Hyades after 700 Myr.

A possible escape route for the "standard" PMS models is if elements, other than Fe, that also form a significant source of opacity in PMS stars (particularly oxygen), are *underabundant* in the Blanco 1 stars compared to a solar mixture. This would mean that, overall, the opacities in the outer envelope of the Blanco 1 stars could be similar to those

in the Pleiades, leading to similar levels of PMS Li depletion (see Piau & Turck-Chièze 2002).

A further issue to address is whether the metallicity determination of E95 can be confirmed. It seems most likely that several of the stars analysed by E95 were *not* cluster members and that as chemical composition was used as a memership discriminator, the overall result might have been biased. Additionally, the temperature scale used in E95 for their atmospheric analyses was considerably hotter than other commonly used calibrations, resulting in a higher overall metallicity estimate (JJ99). Westerlund et al. (1988) found that the cluster was slightly metal deficient on the basis of their Stromgren photometry.

In this paper we analyse high resolution echelle spectroscopy of a sample of candidate F and G stars in Blanco 1. The aims of our study are to confirm whether Blanco 1 really is a very metal-rich open cluster and to find individual abundances for a large range of elements including those important in determining stellar structure such as oxygen, silicon and magnesium.

2 AAT SPECTROSCOPY

2.1 Target selection

Targets were selected to be F- or G-type cluster candidates (to facilitate a differential abundance analysis with respect to the Sun) with low projected rotational velocity and a radial velocity consistent with cluster membership. Four stars were chosen on the basis of information published in JJ99 and a further four from information provided by E95 and J.-C. Mermilliod. (priv. comm). Photoelectric (or photgraphic) Johnson V-band photometry is available for all these targets from Westerlund et al. (1988) or de Epstein & de Epstein (1985), and JHK photometry is available from the 2MASS catalogue (Cutri et al. 2003).

2.2 Observations

High-resolution spectra were collected on 2002 August 25-27 using the 3.9-m Anglo-Australian Telescope (AAT) and a MITLL3 CCD. The University College London Echelle Spectrograph (UCLES) was utilised with the E31 grating to obtain data with R$\simeq$50000 around a central wavelength of 6463Å in order 88. The usual calibration frames were collected, including a reflected solar spectrum (using the Moon) and radial velocity standards. Several exposures were taken of each object, resulting in total integration times of 2400 to 8000 s and signal-to-noise ratios (SNR) of 70-100 per 0.07Å pixel in the central orders.

2.3 Data Reduction

The data were reduced using the Starlink ECHOMOP (Mills et al. 1997) package, which included bias subtraction, flat fielding, subtraction of scattered light and wavelength calibration. Radial velocities (RVs) were measured by cross-correlation of data with wavelengths 5570–5680Å, 6050–6160Å and 6350–6450Å, which contained a number of sharp, neutral metal lines and little telluric contamination. The IAU RV standard star used was HR 6349, with an assumed heliocentric velocity of -17.4 $\mathrm{km\,s^{-1}}$. The calculated RVs are presented (together with other stellar parameters) in Table 1. RV uncertainties quoted are just the standard deviation from cross-correlation of the three separate wavelength ranges. There are additional systematic external errors that probably amount to $\simeq 1\,\mathrm{km\,s^{-1}}$.

3 ANALYSIS

Data analysis was performed using UCLSYN (Smith 1992; Smalley, Smith & Dworetsky 2001), a spectrum synthesis package. Kurucz 1-D, homogeneous, LTE, ATLAS9 (Kurucz 1993) model atmospheres with the mixing-length theory of convection (α=1.25) without overshooting (Castelli, Gratton & Kurucz 1997) were used.

3.1 Atmospheric Parameters

Atmospheric parameters were determined using the spectroscopy. An initial estimate of $T_{\rm eff}$ was obtained from the photometry and this leads to a $\log g$ estimate from a 100 Myr isochrone taken from the evolutionary models of Schaller et al. (1992). We then used measurements of the equivalent widths (EWs) of Fe I lines (see section 3.2) to estimate a microtubulence using the Magain (1986) method. An "ionization balance" locus in the $T_{\rm eff} - \log g$ plane was then found by demanding agreement in the Fe abundances determined using lines arising from both neutral and ionized species. The intercept of this locus with the model isochrone gave a new $T_{\rm eff} - \log g$ estimate and the process was iterated using an atmosphere with a metallicity [M/H] equal to [Fe/H].

This process quickly converged, yielding the parameters quoted in Table 1. Quoted uncertainties in [Fe/H] are solely internal errors and are discussed further in section 4.2. Projected rotation velocities ($v \sin i$) were simultaneously estimated during this process by synthesising the Fe lines with differing $v \sin i$ and minimising chi-squared. The errors quoted for $v \sin i$ in Table 1 are the standard deviation about the average rotational velocity value for each object, based on between 10 and 32 lines.

The atmospheric parameters in Table 1 were used as the basis for determining the abundances of several chemical elements.

3.2 Iron

Lines for study were taken from the list included in Reddy et al. (2003 - hereafter R03), and also from E95. Those lines with $\log gf$ measurements rated B or above in the NIST Atomic Spectra Database were measured in the solar spectrum, and abundances determined. The broadening parameters of Barklem, Piskunov & O'Mara (2000) were used for the van der Waals broadening where available. Adopting $T_{\rm eff}$ = 5780 K, $\log g$ = 4.44 and a microturbulence of 1.21 $\mathrm{km\,s^{-1}}$, an average solar abundance of A(Fe)= 7.44 $\pm$ 0.01 was determined. This value was then assumed in order to obtain astrophysical $\log gf$ values for lines with laboratory $\log gf$ values of lower accuracy.

The EWs were determined by integration of a fitted synthetic spectrum for a total of 34 Fe I and 11 Fe II lines in our reflected solar spectrum. The lines used, their assumed

Table 1. Derived atmospheric parameters for sample stars. Identifiers in **bold** are those used throughout this paper. W identifiers are taken from Westerlund et al 1988; ZS identifiers are those from de Epstein & de Epstein (1985). Effective temperatures derived from photometry and from spectroscopy (see text) are listed.

Object	ZS	$V-K$	T_{V-K} K	T_{spec} K	$\log g$	[Fe/H]	ξ km s^{-1}	RV km s^{-1}	$v \sin i$ km s^{-1}
W64	ZS102	1.77	5430	5440	4.60	-0.04 ± 0.02	1.63	5.1±0.4	5.8±1.4
–	**ZS58**	1.74	5480	5650	4.56	-0.05 ± 0.02	2.21	3.0±1.4	12.0±1.2
–	**ZS141**	1.57	5730	5750	4.53	$+0.09 \pm 0.02$	1.25	4.8±1.4	4.8±1.8
W113	ZS182	1.41	5980	5900	4.50	$+0.09 \pm 0.02$	1.15	4.8±1.2	6.5±1.3
W60	ZS101	1.06	6600	6450	4.38	$+0.11 \pm 0.03$	1.66	5.0±1.1	24.4±2.9
W63	ZS99	1.10	6515	6480	4.38	$+0.05 \pm 0.02$	1.28	2.5±0.7	3.1±1.9
W8	–	1.13	6470	6540	4.38	$+0.09 \pm 0.02$	1.68	3.4±0.3	13.4±2.2
W38	ZS48	1.14	6450	6550	4.37	-0.03 ± 0.02	1.48	4.5±0.5	9.4±2.3
Sun	–			5780	4.44	0.00	1.21	0.0	2

atomic parameters and measured solar EWs are included in Table 2. We then measured the EWs of as many of these lines as possible in the Blanco 1 targets, using synthetic spectra and atmospheric parameters as described in section 3.1. These measurements are also listed (for Fe and all the other elements discussed in this paper) in Table 2, along with all the lines of other elements measured in this paper (see below). A number of lines could not be successfully measured in some of the Blanco 1 targets either as a result of intrinsic weakness, blending with other lines (which is a function of $v \sin i$) or cosmic ray contamination. Mean abundances were calculated for each star, based on estimates of the differential [Fe/H] on a line-by-line basis.

3.3 Oxygen

Oxygen abundances were estimated using the O I lines at 7771-775Å. Each line was synthesised independently to achieve the best fits to our spectra. A differential LTE [O/H] abundance was calculated for each line in each star. Barklem et al. (2000) van der Waals parameters were used and $\log gf$ values were taken from R03. These O I lines are formed high in the atmosphere and are subject to NLTE effects. It would have been better to try and determine oxygen abundances using the weak [O I] 6300Å line, but our data were of insufficient quality to attempt this. Instead we have made a (temperature and gravity dependent) NLTE correction of order 0.1-0.2 dex to the oxygen abundances using the relationship derived for field dwarfs by R03. The NLTE corrections proposed by Gratton et al. (1999) are similar to a few hundredths of a dex. Further comments on the oxygen abundances derived in this manner are deferred to section 4.3.

3.4 Lithium

LTE Li abundances were determined using the Li I resonance lines at 6707.7Å and 6707.9Å. Barklem et al. (2000) van der Waals parameters were used and $\log gf$ values were taken from the NIST database – listed as quality 'A'. The Li feature was synthesised as a doublet; the nearby Fe I line at 6707.4Å was included. No solar measurement was possible due to the inherent weakness of this line in the Sun's Li-depleted photosphere. NLTE corrections were applied using the code provided by Carlsson et al. (1994).

3.5 Carbon, Silicon, Sulphur, Magnesium, Calcium, Titanium and Nickel

Lines for neutral species of these elements were taken from the lists of R03, E95 and Schuler et al. (2003). We chose lines which were likely to be unblended or features where lines of the same species were blended together. Accurate $\log gf$ values were generally not available, so astrophysical $\log gf$ values were obtained by an inverse solar analysis, assuming solar abundances of A(C)= 8.51, A(Si)= 7.62, A(S)= 7.34, A(Mg)= 7.54, A(Ca)= 6.33, A(Ti)= 4.90 and A(Ni)= 6.23, which were derived by R03. van der Waals parameters were taken from Barklem et al. (2000) where available. The final quoted abundances are differential with respect to the assumed solar values.

4 RESULTS

4.1 Chemical Abundances

Table 3 contains the mean abundances for each Blanco 1 target. All results (apart from Li) are differential with respect to the Sun. The quoted uncertainties for each star in this Table are the standard error in the mean abundance from all the features used for that star and element; they do not include the effects of uncertainties in the atmospheric parameters (see section 4.2).

The RVs determined for our targets in Table 1 are reasonably consistent with each other and all lie within 2σ of the mean cluster value deduced by E95 (3.9±0.7 km s^{-1}). Three of our targets (W8, W60, W63) have RV measurements listed in E95 which are reasonably consistent with those reported here. Four targets (W64, W113, ZS58, ZS141) have RVs and $v \sin i$ listed by JJ99 and again they agree within their errors with those found here.

It is worth mentioning that both E95 and Westerlund et al. (1988) doubted the membership credentials of W8. Its distance modulus, derived from Stromgren photometry, is about 0.3 mag lower than most cluster members. The inclusion or not of W8 has no significant effect on our final results for the abundances of Blanco 1. However, we are quite confident on the basis of their RVs that all of these objects are members of Blanco 1 and are either single, long period binary systems or pole-on binary systems. None of the spectra show any signs of contamination from a secondary star.

Table 2. Atomic data and equivalent width measurements

Wavelength	χ_p	log gf	Equivalent widths (mÅ)								
Å	eV		Sun	W113	W38	W60	W63	W64	W8	ZS141	ZS58
	Li I										
6707.760	0.000	-0.002	–	153.1	61.4	92.3	83.4	156.2	25.2	136.0	228.8
6707.910	0.000	-0.299	blended with the above								
	C I										
5380.320	7.685	-1.679	19.9	16.6	38.7	34.9	29.8	13.0	47.3	20.0	15.2
6587.620	8.537	-1.119	13.0	10.2	28.5	31.5	20.3	5.6	32.5	4.2	
7116.960	8.647	-0.886	16.8		34.6	28.7	26.7	5.6	45.7	14.8	
	O I										
7771.944	9.146	0.369	76.2	85.7	150.0	174.1	139.4	53.6	174.0	69.9	
7774.166	9.146	0.223	66.0	68.8	139.3	118.3	119.9	41.2	139.3	59.8	62.8
7775.388	9.146	0.002	50.1	56.5	112.9	116.7	99.6	38.8	119.6	54.4	48.8
	Mg I										
5711.088	4.346	-1.630	114.6	105.0	69.3	81.8	71.9	130.8	81.1	118.9	123.7
6318.717	5.108	-1.813	63.7	53.0	28.1		27.4	75.4			87.8
7657.603	5.108	-1.224	104.5	91.0	59.1	61.9	59.4	107.5	63.9	104.2	142.9
7691.553	5.753	-0.727	136.8	125.5	79.3	93.7	83.3	141.8	93.9	170.6	118.7
	Si I										
6145.016	5.616	-1.453	41.2		25.2	36.5	29.9	32.3	36.8	44.4	39.4
6721.848	5.863	-1.172	50.6	51.6	35.3	38.6	38.6	43.7	40.0	51.9	48.7
6741.628	5.984	-1.595	18.9		10.5		15.7	12.0	17.7	16.2	15.1
6848.580	5.863	-1.703	18.7	16.2	15.2			14.7	13.6	13.5	
7405.772	5.614	-0.683	99.4	92.0	74.6		71.3	87.5	87.6	92.6	82.6
7799.996	6.181	-0.777	70.0	52.2	31.8		36.5	52.1	45.2	55.3	42.3
7918.384	5.954	-0.642	96.9	91.7	65.3		65.6	85.1	61.5	87.7	87.8
	S I										
6052.674	7.866	-0.568	13.5	13.1	21.5	24.2	23.3		27.9		23.6
6757.007	7.866	-1.481	18.4	14.2	31.8	35.7	32.4	11.8	44.2	17.1	18.1
6757.171	7.866	-0.417	blended with the above								
	Ca I										
6166.439	2.521	-1.116	76.3	68.8	39.3	38.5	43.3	89.0	48.1	72.6	87.5
6169.042	2.523	-0.771	101.4	103.4	64.4	65.7	70.3	126.5	77.0	108.9	130.1
6455.598	2.523	-1.304	60.1	59.0	28.4		34.6	71.3	34.9	57.3	79.9
	Ti I										
5219.710	0.021	-2.141	28.3	23.2				49.2		32.2	43.3
5866.452	1.067	-0.743	48.9	40.5	20.1	13.8	13.5	67.1	16.0	44.4	68.5
6091.174	2.267	-0.299	16.0	8.7				22.8			23.9
6126.217	1.067	-1.273	23.2	23.1			5.2		8.1	28.7	39.3
6258.104	1.443	-0.325	53.4	44.3	16.8		19.5	66.1	23.9	56.0	68.0
	Fe I										
5778.455	2.590	-3.397	20.9	20.8				32.1		24.8	
5784.657	3.400	-2.465	29.4				12.4				
5809.217	3.884	-1.589	48.3	46.6	26.1		26.7	63.2	26.9	54.4	60.8
5852.217	4.549	-1.100	42.0	39.4			24.2	49.9	24.6	43.5	48.3
5855.090	4.608	-1.436	21.7				11.7	24.1		21.0	
5858.779	4.220	-2.159	13.2	10.2				17.6			
5859.600	4.549	-0.610	74.4	79.4	48.0	68.5	51.9	90.9	59.5	78.3	82.2
5862.353	4.549	-0.250	89.8	93.7	66.4	82.2	69.8	109.7	75.4		111.1
5956.692	0.859	-4.506	54.9	55.2	11.2			74.9			72.0
6027.050	4.076	-1.170	64.8	66.5	38.6	53.9	42.4	71.4	46.5	63.6	73.4

Wavelength Å	χ_p eV	log gf	Equivalent widths (mÅ) Sun	W113	W38	W60	W63	W64	W8	ZS141	ZS58
	Fe I										
6151.617	2.176	-3.248	48.2	41.9	13.3		19.6			56.7	59.8
6159.368	4.608	-1.779	12.6				7.1		7.5	14.0	
6165.361	4.143	-1.460	44.7	42.9			23.8	49.5	28.7	45.8	
6173.340	2.223	-2.790	67.0	72.5	33.1	43.7	41.4	90.0	46.6	80.8	90.5
6200.314	2.609	-2.285	71.0	78.1	46.3		45.2	98.7	59.7	87.7	111.0
6213.429	2.223	-2.505	84.5	81.1	47.2		53.2	120.7	53.2		
6240.645	3.233	-3.207	50.1				19.3	66.3			
6265.131	2.176	-2.522	82.5	83.3	52.3			115.8	56.7	94.5	122.3
6358.693	0.859	-3.963	80.4	80.5	32.0	41.0		107.2	38.5	95.9	
6436.411	4.186	-2.360	9.7					12.8		12.1	
6481.869	2.279	-2.852	61.2	62.0		42.7		81.9	43.4	68.6	86.8
6518.365	2.830	-2.465	56.0	48.5			30.4		27.3	57.6	69.4
6574.225	0.990	-5.004	26.4					38.6		32.3	
6591.325	4.593	-1.933	9.8	13.9				12.6		14.9	
6608.024	2.279	-3.879	17.3	16.0				27.8		24.4	
6625.021	1.011	-5.340	15.3	12.9				27.7		14.7	
6713.770	4.795	-1.368	21.0	20.3			12.0	21.3		22.5	
6725.353	4.103	-2.107	17.3	19.8				20.1		23.1	
6733.151	4.638	-1.338	26.4	25.4			14.1			30.4	22.3
6739.520	1.560	-4.773	12.0					18.1			
6750.150	2.424	-2.549	69.2	71.4	41.6			112.0		81.0	98.8
6752.705	4.640	-1.130	34.1	35.2	14.9		25.2		24.6	40.5	44.3
6837.016	4.593	-1.644	14.9	15.7					7.1	16.4	19.2
6857.243	4.076	-2.040	21.2	23.8	11.4			33.2		22.9	20.8
	Fe II										
5425.257	3.200	-3.177	45.5		53.2	54.8		38.5	63.6		45.3
5991.376	3.153	-3.563	30.3	36.7	38.0	37.0		22.6	43.4	31.4	26.9
6084.111	3.200	-3.768	20.9	19.5	24.9	38.0			28.9	20.9	18.0
6149.258	3.889	-2.630	35.9	40.9	46.8	49.4	45.7		53.4	37.9	
6247.557	3.892	-2.281	52.0	60.7	69.3	79.7	77.0	47.9	77.8	58.7	52.9
6369.462	2.891	-4.072	18.1	23.9			23.1	13.2	23.1		
6432.680	2.891	-3.520	39.3	49.1	55.6		49.4	35.7	67.0	41.2	
6456.383	3.903	-2.115	46.2	73.3	77.1	87.7	79.7		91.6	68.9	66.1
7222.394	3.889	-3.213	20.0		24.3				34.6		19.2
7449.335	3.889	-3.176	20.0	24.9	28.1	27.1		23.9		28.1	22.0
7515.831	3.903	-3.432	10.6		16.3		22.3				
	Ni I										
5082.339	3.658	-0.489	72.4		50.8		42.8	73.0	50.5		
5094.423	3.833	-1.024	33.9	29.0			11.6	36.2	15.4	30.1	
5115.389	3.834	-0.119	83.3	77.5	53.6	54.4	56.1	101.1	66.0	83.4	86.1
6111.066	4.088	-0.768	38.0		12.7	21.4	16.1		16.8	29.4	30.4
6130.130	4.266	-0.906	23.0	20.4	8.3		7.9	22.1		22.8	
6175.360	4.089	-0.491	52.8	50.2	23.1	26.9	27.6	51.2	29.4	46.7	49.1
6176.807	4.088	-0.235	67.9	59.4	34.5	37.7	37.9	64.9	41.1	62.7	63.8
6204.600	4.088	-1.060	23.6	21.8			10.0	25.0	15.4	19.0	
6378.247	4.154	-0.811	32.4	27.9	12.0	49.8	10.2	29.9	17.5	29.8	
6643.629	1.676	-2.022	96.7	84.7	41.6	31.7	47.3	103.0	53.4		114.7
6772.313	3.658	-0.947	52.4	46.1	22.9		26.7	53.5	31.7	43.4	48.5

4.2 Uncertainties

4.2.1 EW and $\log gf$ *errors*

The errors quoted in Table 3 encapsulate uncertainties in the individual EW measurements and the $\log gf$ values for the lines. These were generally derived from the standard deviation of differental abundances for each line. In cases where only one line was available we used $\delta\mathrm{EW} = (rp)^{0.5}/\mathrm{SNR}$ (where r is the physical width of the line, and p is the pixel size, both in Å) and translated this into an abundance uncertainty. For lithium, the atomic parameters are well understood and introduce additional abundance uncertainties of only $\simeq$0.01 dex.

The scatter in the abundances listed in Table 3 is much larger than the individual error bars. However, we have yet to include a contribution from the uncertain atmospheric parameters for each star.

Table 3. Abundances for target stars. Errors quoted are the standard errors in the measured abundances ($\sigma/\sqrt{n}$). Atmospheric uncertainties (detailed in Table 4) should also be considered. Columns labelled "n" identify the number of features used when obtaining each value. Solar abundances were determined for iron and oxygen, due to the availability of accurate laboratory gfs. In all other cases the solar abundance was fixed at the values listed in the last row. Abundances are quoted differentially with respect to the Sun apart from those for Li. LTE abundances are given and NLTE abundances are also listed for Li and O as discussed in the text.

ID	A(Li) LTE	A(Li) NLTE	n	[C/H]	n	[O/H] LTE	[O/H] NLTE	n	[Mg/H]	n	[Si/H]	n
W64	2.69±0.05	2.65	1	-0.13 ± 0.08	3	$+0.03 \pm 0.06$	-0.09	3	-0.17 ± 0.04	4	-0.14 ± 0.02	7
ZS58	3.31±0.06	3.09	1	-0.05 ± 0.10	1	$+0.05 \pm 0.05$	-0.10	2	-0.07 ± 0.08	4	-0.16 ± 0.04	6
ZS141	2.89±0.05	2.81	1	-0.16 ± 0.17	3	$+0.02 \pm 0.06$	-0.11	3	$+0.01 \pm 0.05$	3	-0.06 ± 0.02	7
W113	3.14±0.05	3.00	1	-0.17 ± 0.01	2	$+0.01 \pm 0.02$	-0.12	3	-0.07 ± 0.02	4	-0.04 ± 0.02	5
W60	3.23±0.12	3.11	1	-0.01 ± 0.06	3	$+0.40 \pm 0.06$	$+0.24$	3	-0.10 ± 0.05	3	$+0.05 \pm 0.05$	2
W63	3.13±0.07	3.03	1	-0.15 ± 0.01	3	$+0.18 \pm 0.02$	$+0.01$	3	-0.14 ± 0.02	4	-0.05 ± 0.04	6
W8	2.60±0.13	2.54	1	$+0.13 \pm 0.02$	3	$+0.35 \pm 0.05$	$+0.19$	3	-0.06 ± 0.05	3	$+0.03 \pm 0.04$	7
W38	3.06±0.10	2.97	1	$+0.00 \pm 0.02$	3	$+0.29 \pm 0.01$	$+0.10$	3	-0.14 ± 0.02	4	-0.07 ± 0.04	7
$A(\mathrm{X})_\odot$				8.51	3	8.89 ± 0.01		3	7.54	4	7.62	7

ID	[S/H]	n	[Ca/H]	n	[Ti/H]	n	[Fe/H]	n	[Ni/H]	n
W64	$+0.04 \pm 0.09$	1	-0.17 ± 0.02	3	-0.16 ± 0.03	4	-0.04 ± 0.02	33	-0.20 ± 0.03	10
ZS58	$+0.24 \pm 0.14$	2	-0.05 ± 0.04	3	$+0.03 \pm 0.03$	5	-0.05 ± 0.02	24	-0.26 ± 0.01	6
ZS141	$+0.00 \pm 0.08$	1	-0.05 ± 0.04	3	$+0.00 \pm 0.05$	4	$+0.09 \pm 0.02$	34	-0.10 ± 0.02	9
W113	-0.12 ± 0.06	2	$+0.04 \pm 0.04$	3	-0.04 ± 0.05	5	$+0.09 \pm 0.02$	35	-0.03 ± 0.01	9
W60	$+0.02 \pm 0.02$	2	-0.15 ± 0.05	2	-0.18 ± 0.12	1	$+0.11 \pm 0.03$	13	-0.15 ± 0.05	6
W63	-0.02 ± 0.01	2	-0.02 ± 0.03	3	-0.12 ± 0.03	3	$+0.05 \pm 0.02$	24	-0.17 ± 0.03	11
W8	$+0.10 \pm 0.04$	2	$+0.02 \pm 0.03$	3	$+0.07 \pm 0.06$	3	$+0.09 \pm 0.02$	25	-0.03 ± 0.03	10
W38	-0.07 ± 0.01	2	-0.11 ± 0.03	3	-0.01 ± 0.10	2	-0.03 ± 0.02	24	-0.17 ± 0.04	9
$A(\mathrm{X})_\odot$	7.34	2	6.33	3	4.90	5	7.44 ± 0.01	43	6.23	11

Table 4. Abundance uncertainties due to estimated atmospheric uncertainties.The quadratic sum of uncertainties due to effective temperature (±100 K), $\log g$ (±0.2), [M/H] (±0.1 dex) and microturbulence (±0.2 $\mathrm{km\,s^{-1}}$) are presented for each star. The first number is the net uncertainty in [X/H], the number in brackets is the net uncertainty in [X/Fe].

	W64	ZS58	ZS141	W113	W60	W63	W8	W38
Fe	0.07	0.06	0.06	0.07	0.06	0.05	0.05	0.05
Li	0.11(0.07)	0.11(0.07)	0.10(0.06)	0.09(0.05)	0.08(0.06)	0.07(0.04)	0.07(0.04)	0.07(0.05)
C	0.10(0.14)	0.09(0.12)	0.09(0.13)	0.09(0.13)	0.08(0.09)	0.07(0.10)	0.07(0.10)	0.07(0.09)
O	0.12(0.16)	0.11(0.14)	0.14(0.18)	0.09(0.14)	0.06(0.09)	0.06(0.10)	0.06(0.09)	0.06(0.09)
Si	0.03(0.07)	0.02(0.05)	0.02(0.05)	0.02(0.05)	0.03(0.05)	0.04(0.03)	0.04(0.04)	0.03(0.04)
S	0.10(0.14)	0.09(0.12)	0.08(0.12)	0.07(0.12)	0.05(0.08)	0.05(0.09)	0.05(0.08)	0.05(0.07)
Mg	0.06(0.06)	0.06(0.06)	0.07(0.07)	0.06(0.05)	0.06(0.06)	0.05(0.04)	0.06(0.05)	0.05(0.05)
Ca	0.10(0.07)	0.09(0.06)	0.09(0.05)	0.09(0.05)	0.06(0.05)	0.06(0.03)	0.06(0.04)	0.06(0.04)
Ti	0.11(0.07)	0.10(0.07)	0.10(0.05)	0.10(0.05)	0.08(0.06)	0.07(0.04)	0.07(0.04)	0.07(0.05)
Ni	0.05(0.02)	0.06(0.02)	0.06(0.02)	0.08(0.06)	0.06(0.04)	0.06(0.02)	0.06(0.03)	0.06(0.04)

4.2.2 Atmospheric parameters

$T_{\rm eff}$ uncertainties are the most important contributor to uncertainties in abundance for all elements except C and S (see below). To estimate a realistic $T_{\rm eff}$ uncertainty we compare $T_{\rm eff}$ derived from the spectroscopy with that derived using the relationship between $T_{\rm eff}$ and $V-K$ colour index from Alonso, Arribas & Martinez-Rogers (1996). A small correction was made to the 2MASS K photometry (using formulae in Carpenter 2001) in order to convert it to the Carlos Sanchez Telescope (TCS) system used by Alonso et al. A reddening $E(V-K) = 0.055$ is assumed, corresponding to $E(B-V) = 0.02$ for the cluster determined by Westerlund et al. (1988). We chose this colour index because (i) the data is available for all our targets; (ii) it is very sensitive to $T_{\rm eff}$; (iii) it is almost independent of the photospheric composition and gravity and (iv) is unlikely to be significantly affected by chromospheric activity (Stauffer et al. 2003). This latter point could be important in a young cluster like Blanco 1 where chromospheric activity can lead to blue excesses and possible problems when using $B-V$ or Stromgren photometry to determine $T_{\rm eff}$ or $\log g$.

$T_{\rm eff}$ values derived from the $V-K$ photometry and from the spectroscopy are listed in Table 1. A comparison of the two $T_{\rm eff}$ determination methods yields a mean difference $(T_{V-K} - T_{\rm spec})$ of -13 ± 36 K with a standard deviation of 102 K. As the precision of the photometry leads to uncertainties of only $\simeq 50$ K in T_{V-K} then most of this scatter must be due to $T_{\rm spec}$ uncertainties of $\simeq 100$ K. The agreement between the two scales lends some confidence that there are

no major systematic uncertainties in the temperatures we have used and no problems with our ionization balance temperatures caused by possible NLTE overionization effects in the Fe II lines – which may become more apparent in cooler stars (< 5500 K – see Schuler et al. 2003; Allende-Prieto et al. 2004). In addition we have checked plots of abundance from the Fe I lines versus lower excitation potential and none show any significant trends that would indicate a $T_{\rm eff}$ error of more than ± 150 K.

Having used a cluster isochrone in the $T_{\rm eff} - \log g$ plane to determine $\log g$, then an uncertainty in $T_{\rm eff}$ naturally leads to an uncertainty in $\log g$. In fact this uncertainty is small, but we choose (conservatively) to allow $\log g$ to vary by ± 0.2. Because the isochrone $\log g$ varies very slowly with $T_{\rm eff}$, the uncertainties in $T_{\rm eff}$ and the assumed $\log g$ errors are essentially uncorrelated. The $\log g$ uncertainty is dominant for the C and S abundance determinations, but less important than the $T_{\rm eff}$ uncertainties for all the other elements. We adopt conservative microturbulence uncertainties of $\pm 0.2\,{\rm km\,s^{-1}}$ and atmospheric metallicity uncertainties of ± 0.1 dex. These contribute 0.02-0.03 dex abundance uncertainty to the O, C and Fe abundances but add a negligible amount to the overall error budget for the other elements.

Table 4 details the quadratic sum of uncertainties in [X/H] due to the atmospheric parameter uncertainties, making the assumption that the different sources of error are independent. These have been estimated by repeating the abundance analysis for each star/element after perturbing their atmospheric parameters. We have also estimated total uncertainties on [X/Fe]. These are smaller or larger than corresponding uncertainties in [X/H] depending on whether changes in the atmospheric parameters cause changes in the derived abundances which are in the same (e.g. Ca, Ni) or contrary (e.g. C, O, S) direction to those in the Fe abundance. The errors in Table 4 should be combined in quadrature with those quoted in Table 3 in order to obtain the overall (internal) errors on the abundances for each star.

4.3 Mean cluster abundances

With the internal uncertainties established, Table 5 lists the weighted mean abundances for Blanco 1 in the form of [X/H] and [X/Fe], using all eight stars and the quadratic sum of the uncertainties presented in Tables 3 and 4. We quote the standard errors in the weighted mean and also the reduced chi-squared (for 7 degrees of freedom) of the weighted mean fitted to the data and the probability that a chi-squared of this size could arise given the quoted errors. These results are graphically presented in Fig. 1.

For Fe, C, Mg, S, Ca, Ti and Ni the scatter in the [X/H] abundance measurements are consistent with the estimated uncertainties, with reasonably low reduced chi-squared values. This lends confidence in our methods and uncertainty estimates for these elements and also suggests that any star-to-star scatter of abundances within the cluster is smaller than the uncertainties estimated for each star. However, there are three elements (Li, O, Si) where a high reduced chi-squared is found. This could indicate either (i) that the elemental abundance genuinely varies from star-to-star, (ii) that the abundance uncertainties have been underestimated or (iii) that there is an apparent trend of abundance with $T_{\rm eff}$ arising from an inadequate treatment of the atmosphere, NLTE effects or the temperature scale.

For Li it is very likely that explanation (i) applies. Li is known to be depleted in many cooler ($T_{\rm eff} < 5800$ K) stars among Blanco 1 and the similarly aged Pleiades (e.g. Soderblom et al. 1993; JJ99). This could account for low Li abundances in ZS141 and W64. Of more interest is the low Li abundance of W8 with a $T_{\rm eff} \simeq 6500$ K and a NLTE A(Li) which is about 0.5 dex lower than the three other stars in the sample with similar $T_{\rm eff}$. This star also has a lower Li abundance than any similar stars in the Pleiades. It is tempting to speculate that this marks the development of the "Boesgaard gap" (Boesgaard & Tripicco 1986) of Li-depleted F-stars that is clearly seen in the older (700 Myr) Hyades cluster. Steinhauer & Deliyannis (2004) claim that the gap starts to form as early as 150 Myr on the basis of Li-depleted F-stars in the open cluster M35. However, the membership of W8 in Blanco 1 may still be problematic (see section 4.1). If the membership of W8 can be confirmed and further examples of Li-depleted F-stars were found in Blanco 1 this would probably indicate that the cluster is a little older than the Pleiades.

The O abundances of the Blanco 1 stars show a clear trend with $T_{\rm eff}$. The group of 4 cooler stars have a mean $[{\rm O/H}]_{\rm NLTE}$ that is 0.20 ± 0.05 dex *lower* than the 4 stars with $T_{\rm eff} > 6000$ K and this is responsible for the high reduced chi-squared value in Table 5. Blanco 1 is a young cluster and its stars are magnetically active as a consequence of rapid rotation and dynamo action. It has been noted by previous workers that it can be difficult to obtain oxygen abundances in chromospherically active stars using the O I triplet lines. Spuriously high oxygen abundances might be obtained, which are not adequately dealt with by NLTE corrections similar to those we adopt here. Such abundance over-estimates seem to increase with chromospheric activity (Morel & Micela 2004; Schuler et al. 2004). However, both Morel & Micela and Schuler et al. suggest that this effect, (which is possibly attributable to overionisation/excitation in the upper atmosphere), *does not* seriously compromise oxygen abundances determined from the triplet lines for stars with $T_{\rm eff} > 5500$ K. This suggestion needs further testing with high signal-to-noise observations of the weak [OI] 6300Å feature in chromospherically active F and G dwarfs. We note here that the sample stars presented in this work are mostly slow rotators (although a low inclination angle could mask pole-on rapid rotators), and that the derived NLTE oxygen abundances for the cooler stars are *lower* than for the hotter stars, suggesting chromospheric activity is not to blame for the trend we see. In any case it seems that the NLTE corrections are not entirely satisfactory and we judge it prudent to add a further systematic uncertainty of ± 0.1 dex to the mean cluster O abundances.

The Si abundances appear to follow a similar $T_{\rm eff}$ trend to the O abundances albeit not so significant. Adding a slope to the abundance versus $T_{\rm eff}$ relationship yields a gradient only 2 sigma above zero (compared with 4 sigma for O). We note that the strengths and excitation potentials of the Si lines we have used are similar to, although higher on average, than those of Mg where a small chi-squared and no trend with $T_{\rm eff}$ is observed. Instead it could be that the Si abundance measurements, which are the most precise of all the elements considered here, highlight additional sources

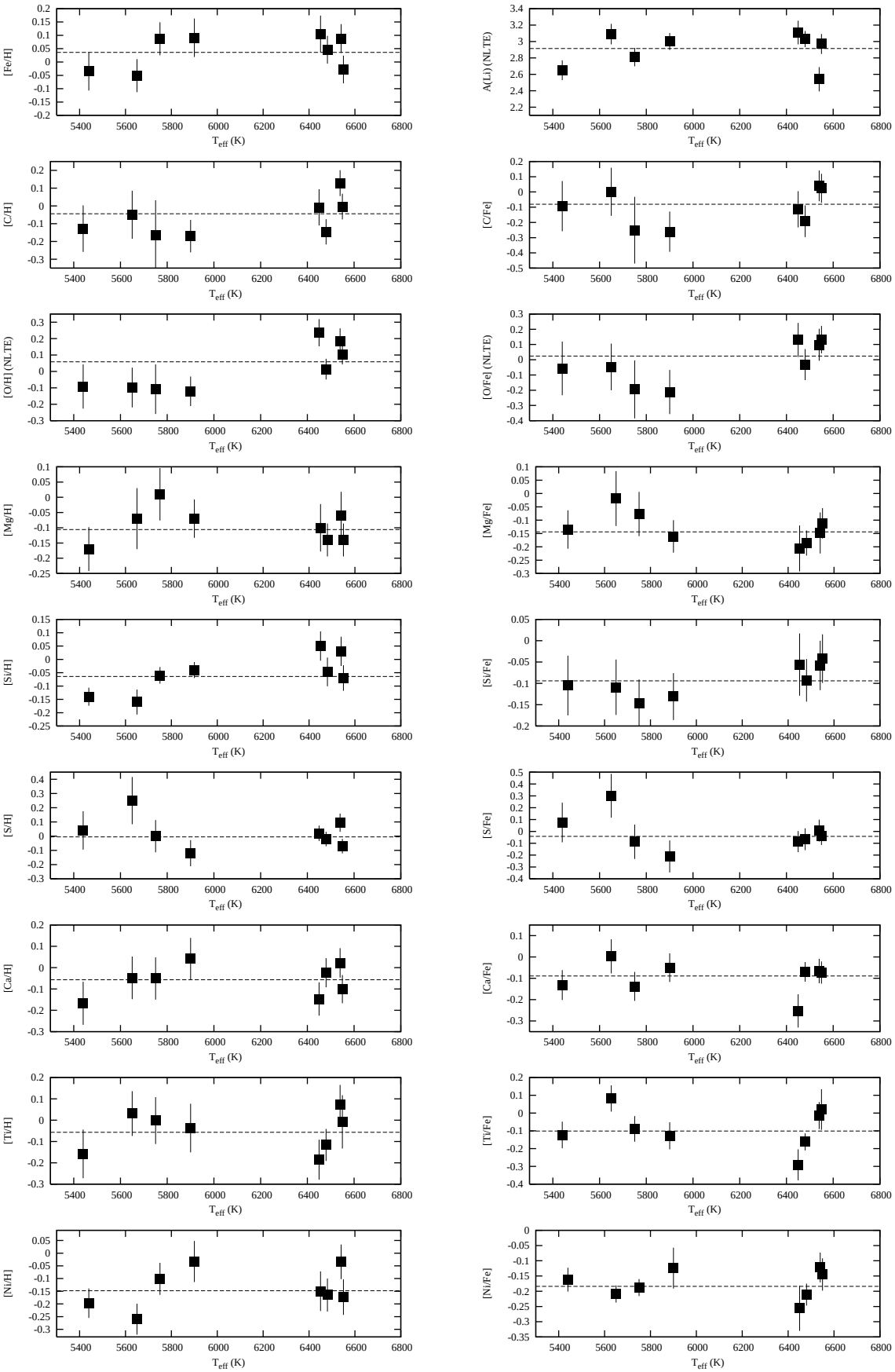

Figure 1. Abundances and abundance ratios versus $T_{\rm eff}$. Dashed lines indicate weighted means.

Table 5. Weighted mean abundances for Blanco 1, based on observations in this work. Errors are the (weighted) standard error and do not include any external uncertainties due to choice of atmospheric model or systematic shifts in the $T_{\rm eff}$ scale.

Element	[X/H]	$\Delta T = +100\,$K	χ^2_ν	$P(>\chi^2)$	[X/Fe]	$\Delta T = +100\,$K	χ^2_ν	$P(>\chi^2)$
Fe	$+0.04 \pm 0.02$	$+0.04$	1.10	0.36				
A(Li)	$+2.92 \pm 0.04$	$+0.08$	2.59	0.01				
C	-0.04 ± 0.04	-0.05	1.68	0.11	-0.08 ± 0.04	-0.09	0.95	0.47
O†	$+0.06 \pm 0.11$	-0.04	2.31	0.02	$+0.02 \pm 0.11$	-0.09	1.08	0.38
Mg	-0.11 ± 0.02	$+0.05$	0.60	0.76	-0.14 ± 0.02	$+0.00$	0.55	0.80
Si	-0.06 ± 0.02	$+0.02$	2.44	0.02	-0.09 ± 0.02	-0.03	0.41	0.89
S	$+0.00 \pm 0.03$	-0.03	1.20	0.30	-0.04 ± 0.04	-0.08	0.88	0.52
Ca	-0.06 ± 0.03	$+0.07$	0.79	0.60	-0.09 ± 0.02	$+0.02$	1.06	0.39
Ti	-0.06 ± 0.03	$+0.09$	0.92	0.49	-0.10 ± 0.03	$+0.05$	2.16	0.04
Ni	-0.15 ± 0.03	$+0.05$	1.38	0.21	-0.18 ± 0.01	$+0.01$	0.80	0.59

† O abundance errors include ± 0.1 in NLTE corrections.

of error not yet included (for instance atmospheric inhomogeneities or a $T_{\rm eff}$-dependent error in the $T_{\rm eff}$ scale). If so, it would only have to amount to an additional 0.03 dex uncertainty on each stellar Si abundance to reduce the chi-squared to acceptable (> 10 per cent probability) levels. This level of extra uncertainty would have a negligible impact on the mean abundances for the other elements.

It is interesting to note that none of the [X/Fe] abundance ratios show any significant evidence for either trends with $T_{\rm eff}$ or that the abundance errors are underestimated. This perhaps indicates that any additional sources of error in [X/H] are mirrored by similar errors in [Fe/H].

4.4 External Errors

Before comparing our Blanco 1 abundances with other published results for cluster and field stars or using these results as inputs to stellar evolution calculations, external errors must be considered. Systematic shifts in the abundances of our target stars could be caused by uncertainties in the way we calibrated the $T_{\rm eff}$ scale, dependence on the atmospheric models, the uncertain age of the cluster etc.

The sensitivity to differing atmospheric models of differential abundance analyses on F/G stars has been investigated by Allende-Prieto et al. (2004). They found that changing between Kurucz ATLAS9 and MARCS (Gustafsson et al. 1975) models can alter differential [X/H] abundances by up to 0.05 dex. The largest changes were found amongst abundances derived from lines with high excitation potential, such as C, O and S. Likewise, R03 showed that differential [X/H] abundances altered by only a few hundredths of a dex when changing between ATLAS9 models with and without convective overshoot, but that differences in [X/Fe] were negligible. R03 also showed that their [X/Fe] values agreed well (to within a few hundredths of a dex) with those of Chen et al. (2002) for stars in common, where the latter authors had used a similar $T_{\rm eff}$ calibration but MARCS models. We do not consider these model-dependent uncertainties any further but the reader should be aware of them.

The effects of a shift in the $T_{\rm eff}$ scale can be estimated by arbitrarily increasing $T_{\rm eff}$ for all the stars by 100 K – which represents a likely level of uncertainty in the ionization balance calculations and the empirical $T_{\rm eff}$ scales of Alonso et al. (1996)[1]. The results are listed in Table 5 for both [X/H] and [X/Fe]. Such a change results in a mean [Fe/H] change of +0.04 dex and between +0.02 and +0.09 dex for Si, Mg, Ca, Ti, Ni – hence [Si/Fe] etc. are changed by less than ± 0.05 dex and [Mg/Fe], [Ni/Fe] by negligible amounts. [C/H], [O/H] and [S/H] behave in the opposite sense, with mean abundances *decreasing* by 0.03 to 0.05 dex and hence [C/Fe], [O/Fe] and [S/Fe] decrease by 0.08 to 0.09 dex.

Systematic shifts in the $\log g$ calibration are also possible. If the cluster was a little older or younger or we were to adopt other evolutionary models then $\log g$ might change, at most, by ± 0.2 dex. Potentially this could change C abundances by ± 0.06 dex, O abundances by ± 0.04 dex and Mg and Ca abundances by ∓ 0.03 dex. Other elements are negligibly affected.

4.5 Comparison with Edvardsson et al. (1995)

E95 also calculated mean abundances (differentially with respect to the Sun) for Blanco 1. Their methods differed from ours in that they generally used fewer lines and adopted $T_{\rm eff}$ and $\log g$ values derived from Stromgren photometry using the calibrations described in Edvardsson et al. (1993).

E95 obtain a mean cluster [Fe/H] (on the basis of four F stars) of $+0.23 \pm 0.01$, [Ni/H] of $+0.10 \pm 0.02$, [Si/H] of $+0.13 \pm 0.05$ and [Ca/H] of $+0.19 \pm 0.03$. Their estimated external errors were about ± 0.1 dex.

Our results for [Ni/Fe], [Si/Fe] and [Ca/Fe] match those of E95 reasonably well. This is reassuring as we claimed in the last section that these ratios are quite robust to changes in models and $T_{\rm eff}$ scales. However, our overall abundances are lower by 0.18-0.29 dex, which is several times larger than our estimates of the internal errors and the external errors quoted by us or E95.

A comparison of the $\log gf$ values and calibrating solar EWs for lines in common between the two studies reveal no large or systematic discrepancies. The root cause of the abundance differences appears to be in the $T_{\rm eff}$ scale. We have three stars in common with the E95 study – W8 ($[{\rm Fe/H}]_{\rm E95} = +0.23 \pm 0.02$), W60 ($[{\rm Fe/H}]_{E95} = +0.02 \pm 0.03$

[1] A revision of the Alonso et al. (1996) calibrations has been published by Ramírez & Meléndez (2005). However, their $V-K$–$T_{\rm eff}$ relation yields temperatures only 20-30 K hotter for our stars.

– which E95 discount as a cluster member on the basis of its abundance!) and W63 ($[\mathrm{Fe/H}]_{\mathrm{E95}} = +0.21 \pm 0.01$) – but in our analysis these stars are cooler by 225 K, 150 K and 420 K respectively. If E95 had adopted the atmospheric parameters we have used, then their [Fe/H] for W8 and W63 would have been in excellent agreement with our results. The [Fe/H] of W60 would have been about 0.15 dex lower, but E95 explain that the rotational broadening of this star may have caused them to underestimate the EWs (and hence abundance), a problem which our spectral synthesis technique avoids.

In deciding what the overall abundances are in Blanco 1 the question of the adopted T_{eff} scale is crucial. E95 chose to use temperatures indicated by the Stromgren photometry and the Edvardsson et al. (1993) calibration despite the fact that their own spectroscopy – in the form of trends of abundance versus excitation potential and the ionization balance – indicated that significantly lower temperatures were warranted. Other authors (R03) have also noted that the Edvardsson et al. (1993) T_{eff} scale is 100–150 K hotter than that deduced from Stromgren photometry and the Alonso et al. (1996) or Saxner & Hammarback (1985) calibrations. We further note that for the Blanco 1 stars considered here, and by E95, that temperatures found from Stromgren photometry and the Alonso et al. (1996) calibrations are systematically hotter than those based on $V-K$ by a further $\simeq 150$ K, but are less precise (about ± 120 K) and are dependent on metallicity and gravity. For these reasons and because we are able to achieve ionisation balance at a similar temperature to that indicated by the $V-K$ photometry, we believe our abundances are more robust. We do concede that an upward correction to our T_{eff} scale of $\simeq 100$ K is still possible and the consequences of such a shift were examined in section 4.4.

4.6 Comparison with Jeffries & James 1999

Four of our cooler targets (W64, W113, ZS58, ZS141) were observed by JJ99. The temperatures derived there were based on the $B-V/T_{\mathrm{eff}}$ calibration of Bohm-Vitense (1981) with an extra metallicity-dependent term. These temperatures are only 16–116 K hotter than the spectroscopically derived temperatures in this paper, but had JJ99 used the metallicities derived here rather than *assuming* a mean cluster metallicity of +0.14 then even better agreement would be obtained. Only Li abundances were calculated by JJ99, based on curves of growth presented by Soderblom et al. (1993) and also corrected for NLTE effects using the code of Carlsson et al. (1994). The difference between the J99 NLTE Li abundances and those in Table 3 is (-0.01 ± 0.05) dex.

5 DISCUSSION

5.1 The abundance mix in Blanco 1

The main results of our analysis are:

(i) The overall metallicity is much lower than found in the previous study by E95. This is mainly due to our adoption of a lower T_{eff} scale.

(ii) We confirm the tentative findings of E95, that [Ni/Fe] and [Si/Fe] are significantly sub-solar. Furthermore, after considering the possible sources of internal and external error, we also find that [Mg/Fe] and [Ca/Fe] are sub-solar. The same sub-solar trend is indicated for [C/Fe], [S/Fe] and [Ti/Fe] but at a lower level of significance. In fact the only solar abundance ratio is that for [O/Fe], but the error bar is large enough that it may also be consistent with the ratios for the other alpha elements.

The abundance pattern in Blanco 1 is very unusual. [Ni/Fe], [Mg/Fe], [Si/Fe] and [Ca/Fe] are all derived from multiple lines with moderate excitation potentials and line strengths. These ratios are quite robust to systematic errors and have been measured in a similar way in several large studies of field dwarfs (Edvardsson et al. 1993; Chen et al. 2002; R03; Allende-Prieto 2004). Yet none of these studies contain *any* stars with [Ni/Fe] or [Mg/Fe] as low as we find for Blanco 1, and stars that are underabundant in the other alpha elements are rare. On the other hand there is at least one other open cluster, M34, which has $[\mathrm{Ni/Fe}] = -0.12 \pm 0.02$ and $[\mathrm{Mg/Fe}] = -0.10 \pm 0.02$ derived using spectroscopic methods similar to those used here (Schuler et al. 2003).

The underabundance of both Ni and the alpha elements in Blanco 1 may perhaps be better considered as an excess of Fe and leaves us with two puzzles. The first is that R03 claim that at a given [Fe/H] there is only a very narrow ($\leqslant 0.05$ dex) spread in [Ni/Fe] and the other abundance ratios discussed here. This is evidence that at any given time, the ISM in star forming regions of the galactic disc has been thoroughly mixed and is locally homogeneous. Blanco 1 is quite exceptional from this point of view; the gas from which it formed may not have been well mixed with the bulk of the galactic disc ISM. It should be noted however that the spectroscopic surveys of field F and G stars are quite limited in the distances that they probe, although they span a range of galactic birth site radii of a few kpc.

The second puzzle is the nature of the abundance anomalies in Blanco 1. The main sources of Fe in the ISM are supernovae of types I and II or possibly hypernovae. SN II and hypernovae invariably produce super-solar yields of [Si/Fe] (and the other alpha elements). The relative yields of iron-peak elements are somewhat dependent on the detailed supernova physics but recent models suggest that the Ni/Fe ratio is somewhere between 0.75 and 2.0 times the solar value (Nakamura et al. 2001; Hoffmann, Woosley & Weaver 2001). On the other hand SN Ia explosions produced by accretion onto a massive white dwarf produce little Mg but have ejecta with Ni/Fe ratios that are greater than 1.5 times the solar value (e.g. Iwamoto et al. 1999; Travaglio et al. 2004). It is therefore difficult to understand how the material from which Blanco 1 formed could appear depleted of alpha elements *and* Ni with respect to Fe.

The solution to these puzzles (as first noted by E95) could be connected with a very unusual formation history for Blanco 1. The cluster lies at high galactic latitude ($b = -79^{\circ}$) and is some 240 pc below the galactic plane. This is far in excess of the maximum scale height achieved by similarly young field stellar populations or open clusters. E95 speculated that Blanco 1 may have formed in the shocked gas of a high velocity cloud during a collision with the galactic plane ISM (Comerón & Torra 1994). In any case, its undoubtedly peculiar trajectory may mean that the material from which Blanco 1 originated had travelled some distance

and did not have the chance to homogenise with the local galactic disc ISM.

Perhaps the ISM from which Blanco 1 formed was enriched by one or two peculiar supernovae? In the literature there are some models of "delayed detonation" SN Ia, produced by the merger of two white dwarfs, which do produce more Fe than Ni (Khokhlov, Müller & Höfflich 1993). If, as suggested by E95, Blanco 1 formed from a $3000\,M_\odot$ cloud, then a single such event could pollute the cloud sufficiently to raise [Fe/H] by 0.1 dex, but would only decrease [Ni/Fe] by 0.03 dex, which does not seem sufficient.

5.2 Implications for Li depletion

Li in Blanco 1 was investigated by JJ99 who wished to determine whether its higher metallicity with respect to (for instance) the Pleiades would result in increased levels of PMS Li burning and depletion, as predicted by standard evolutionary models. That no significant differences were seen in the Li-depletion patterns of Blanco 1 and the Pleiades indicated problems for the standard models and that a mechanism which inhibited Li-depletion in Blanco 1 was required.

JJ99 assumed a mean metallicity [M/H] of +0.14 for Blanco 1. In this paper we have determined a lower value; furthermore we have found that if anything, the abundances of other alpha elements which are an important source of radiative opacity in the envelopes of PMS stars, primarily O, Mg and Si (Piau & Turck-Chiéze 2002) are even lower. The Pleiades has [Fe/H] $= -0.034 \pm 0.024$ (Boesgaard & Friel 1990), [O/H] $= +0.02 \pm 0.10$ (based on the O I triplet measurements of stars with $T_{\rm eff} > 5500$ K in Schuler et al. 2004 and applying the same NLTE corrections as in this work), [Si/Fe] $= +0.09$, [Ca/Fe] $= +0.07$ and [Ni/Fe] $= +0.02$ (Wilden et al. 2002). Thus the mean metallicity and hence radiative opacities in Blanco 1 are probably quite similar to those in the Pleiades.

The predictions of standard models are therefore adequate to explain why the Li depletion patterns of cool stars in the Pleiades and Blanco 1 are indistinguishable. However the same models do have other problems (they deplete too much Li overall and cannot explain the scatter in Li abundances for young cluster K-stars – e.g. Jeffries 2005) and there are other sets of clusters with similar ages that show almost identical levels of Li-depletion despite their differing (spectroscopically determined) [Fe/H] values (e.g. Jeffries et al. 2002; Sestito, Randich & Pallavicini 2004). A thorough spectroscopic investigation of the individual elemental abundances of these clusters is certainly warranted.

6 SUMMARY

We have determined elemental abundances for a group of eight F- and G-type stars that are good candidate members of the young open cluster Blanco 1. The mean cluster [Fe/H] is $0.04 \pm 0.02 \pm 0.04$[2], considerably lower than a previous spectroscopic determination by Edvardsson et al. (1995). The difference is mainly due to the adoption of a significantly cooler $T_{\rm eff}$ scale in this paper, which we argue is more consistent with both photometric and spectroscopic indicators.

We find that Blanco 1 has significantly subsolar values of [Si/Fe] $(= -0.09 \pm 0.02 \pm 0.03)$ and [Ni/Fe] $(= -0.18 \pm 0.01 \pm 0.01)$ and extend this trend to include [Mg/Fe] $(= -0.14 \pm 0.02 \mp 0.03)$, [Ca/Fe] $(= -0.09 \pm 0.02 \pm 0.03)$ and [Ti/Fe] $(= -0.10 \pm 0.03 \pm 0.05)$. The abundance ratios of [O/Fe], [C/Fe] and [S/Fe] are derived from high excitation potential lines and subject to larger uncertainties. They may be consistent with the underabundances seen for the other elements but could also assume solar values.

The combination of a deficit of both Ni and the alpha elements Mg and Si with respect to Fe is difficult to explain with published models of SN Ia and SN II. These subsolar abundance ratios are also very unusual when compared with samples of nearby stars that have had their abundances measured using similar techniques. This may indicate that the material from which Blanco 1 formed was not well mixed with the ISM of the galactic disc and may have been polluted by one or two unusual supernova events. The large distance of Blanco 1 from the galactic disc combined with its youth also point to an unusual formation history.

Our revised determination of the Blanco 1 abundances could explain why the Li depletion pattern observed among its G- and K-type members is indistinguishable from those in the Pleiades. The overall radiative opacities and hence convection zone properties at a given mass will be very similar in the two clusters. Unfortunately, our lower revised abundances for Blanco 1 also mean it may not be such a fruitful place to look for short-period exoplanets.

ACKNOWLEDGMENTS

This research has made use of NASA's Astrophysics Data System, and the SIMBAD Astronomical database and VizieR service hosted by CDS. We thank the director and staff of the Anglo Australian Observatory for assisting with the success of our observations.

REFERENCES

Allende-Prieto, C., Barklem, P.S., Lambert, D.L., Cunha, K. 2004, A&A, 420, 183
Alonso, A., Arribas, S. Martinez-Roger, C. 1996, A&A, 313, 873
Barklem, P., Piskunov, N., O'Mara, B. 2000, A&AS, 142, 467
Boesgaard, A.M., Friel, E. 1990, ApJ, 351, 480
Boesgaard, A.M., Tripicco, M.J. 1986, ApJ, 302, L49
Carlsson, M., Rutten, R.J., Bruls, J.H.M.J., Shchukina, N.G. 1994, A&A, 288, 860
Carpenter, J. 2001, AJ, 121, 2851
Castelli, F., Gratton, R., Kurucz, R.L. 1997, A&A, 318, 841
Chen, Y.Q., Nissen, P.E., Zhao, G., Zhang, H.W., Benoni, T. 2002, A&AS, 141, 491
Comerón, F., Torra, J. 1994, A&A, 281, 35
Cutri, R.M. et al. 2003, Explanatory supplement to the 2MASS All Sky data release, http://www.ipac.caltech.edu/2mass/

[2] Here and below, the first uncertainty is an internal error incorporating statistical errors and uncertainties in atmospheric parameters for each star. The second uncertainty is a systematic external error and incorporates possible errors of 100 K in the adopted temperature scale and 0.2 in the adopted $\log g$ values (see section 4.4).

de Epstein, A., de Epstein, I. 1985, AJ, 90, 1211
Edvardsson, B., Andersen, J., Gustafsson, B., Lambert, D.L., Nissen, P.E. Tomkin, J. 1993, A&A, 275, 101
Edvardsson, B., Pettersson, B., Kharrazi, M., Westerlund, B. 1995, A&A, 293, 75 (E95)
Gratton, R.G. Carretta, E., Eriksson, K., Gustafsson, B. 1999, 350, 955
Grevesse, N., Sauval, A.J. 1998, Space Sce. Rev., 85, 161
Gustafsson, B., Bell, R.A., Eriksson, K., Nordlund, øA. 1975, A&A, 42, 407
Hoffman, R.D., Woosley, S.E., Weaver, T.A. 2001, ApJ, 549, 1085
Iwamoto, K., Brachwitz, F., Nomoto, K., Kishimoto, N., Umeda, H., Hix, R.W., Thielemann, F.-K. 1999, ApJS, 125, 439
Jeffries, R.D. 2005, in Chemical abundances and mixing in stars in the Milky Way and its satellites, eds. L. Pasquini, S. Randich, ESO Astrophysics Symposium (Springer-Verlag) in press
Jeffries, R.D., James, D.J. 1999, ApJ, 511, 218 (JJ99)
Jeffries, R.D., Totten, E.J., Harmer, S., Deliyannis, C.P. 2002, MNRAS, 336, 1109
Khokhlov, A., Müller, E., Höfflich, P. 1993, A&A, 270, 223
Kurucz, R.L. 1993, Kurucz CD Rom, Atlas 9, SAO, Cambridge
Magain, P. 1986, A&A, 163, 135
Meynet, G., Mermilliod, J.C., Maeder, A. 1993. A&AS, 98, 477
Mills, D., Webbb, J., Clayton, M. 1995, Starlink User Note 152.4
Morel, T., Micela, G. 2004, A&A, 423, 677
Nakamura, T., Umeda, H., Iwamoto, K., Nomoto, K., Hashimoto, M., Hix, W.R., Thielemann, F.-K. 2001, ApJ, 555, 880
Panagi, P.M., O'Dell, M.A., Collier Cameron, A., Robinson, R.D. 1994, A&A, 292, 439
Perry, C.L., Walter, D.K., Crawford, D.L. 1978, PASP, 90, 81
Piau, L., Turck-Chièze, S. 2002, ApJ, 566, 419
Pillitteri, I., Micela, G., Sciortino, S., Damiani, F., Harnden, F.R. Jr. 2004, A&A, 421, 175
Pillitteri, I., Micela, G., Sciortino, S., Favata, F. 2003, A&A, 399, 919
Ramírez, I., Meléndez, J. 2005, ApJ, 626, 465
Reddy, B.E., Tomkin, J., Lambert, D.L., Allende Prieto, C. 2003, MNRAS, 340, 304 (R03)
Santos, N.C., Israelian, G., Mayor, M. 2004, A&A, 415, 1153
Saxner, M., Hammarback, G. 1985, A&A, 151, 372
Schaller, G., Schaller, D., Meynet, G., Maeder, A. 1992, A&AS, 96, 269
Schuler, S.C., King, J.R., Fischer, D.A., Soderblom, D.R., Jones, B.P. 2003, AJ, 125, 2085
Schuler, S.C., King, J.R., Hobbs, L.M., Pinsonneault, M.H. 2004, ApJ, 602, L117
Sestito, P., Randich, S., Pallavicini, R. 2004, A&A, 426, 809
Smalley, B., Smith, K., & Dworetsky, M. 2001, UCLSYN User Guide, incorporating BINSYN and TELSYN, 3.1 edition
Smith, K. 1992, Ph.D. Thesis, University of London
Shortridge, K., Meyerdicks, H., Currie, M. et al. 1999, Starlink User Note 86.17
Soderblom, D.R., Jones, B.F, Balachandran, S., Stauffer, J.R., Duncan, D.K., Fedele, S.B., Hudon, J.D. 1993, AJ, 106, 1059
Stauffer, J.R., Jones, B.F., Backman, D., Hartmann, L.W., Barrado y Navascués, D., Pinsonneault, M.H., Terndrup, D.M., Muench, A.A. 2003, AJ, 126, 833
Steinhauer, A., Deliyannis, C.P. 2004, ApJ, 614, L65
Travaglio, C., Hillebrandt, W., Reinecke, M., Thielemann, F.-K. 2004, A&A, 425, 1029
Westerlund, B.E., Garnier, R., Lundgren, K., Petterson, B., Breysacher, J. 1988, A&AS, 76, 101
Wilden, B.S., Jones, B.F., Lin, D.N.C., Soderblom, D.R. 2002, AJ, 124, 2799

This paper has been typeset from a TEX/ LATEX file prepared by the author.